

# Target Tracking in Non-Gaussian Environment

**N Shantha Kumar**  
Scientist, FMC Division  
NAL, Bangalore 560 017  
E-mail: [nskumar@css.nal.res.in](mailto:nskumar@css.nal.res.in)

**Sudesh Kumar Kashyap**  
Scientist, FMC Division  
NAL, Bangalore 560 017  
E-mail: [sudesh@css.nal.res.in](mailto:sudesh@css.nal.res.in)

## Abstract

*Masreliez filter which is a Kalman type of recursive filter is implemented and validated. The main computation in Masreliez filter is to evaluate the score function which directly influences the estimates of the target states. Scalar approximation for score function evaluation is extended to vector observations, implemented and validated. The simulation studies have shown that the performance of the Masreliez filter is relatively better than that of the conventional Kalman filter in the presence of significant glint noise in the observation.*

**Keywords:** Target tracking, Glint noise, Kalman filter, Masreliez filter, Score function

## 1 Introduction

It is well known that Kalman filter gives optimal solution when the various uncertainties such as process noise and measurement noise are Gaussian. But the same filter gives sub-optimal solution when the uncertainties are non-Gaussian. In radar tracking system, measurement noise often shows non-Gaussian distribution due to random wandering of the apparent measured position of a target due to interference of reflections from different elements of the target. This is referred to as the glint noise. Filtering in non-Gaussian environment has been studied by many researchers. Masreliez[1] introduced a nonlinear score function as the corrective term in the state estimation and the results are often nearly optimal.

However, the implementation of score function is difficult except for simple cases. Wu[2,3] developed an efficient approximation method for score function evaluation. This method employs an adaptive normal expansion to expand the score function and truncates the higher order terms in the expanded series. It is shown in [2] that the approximation is satisfactory and the method is simple and practically feasible. However, the approach developed in [2] is easy to implement for the scalar observation and often one has to handle vector observation in radars.

In this paper, the approximate score function evaluation method mentioned in [2] is extended to radar vector observation. Two cases are considered for validation. In

the first case, the state model is proposed in cartesian coordinate frame and the observations are developed into three independent components by converting range, azimuth and elevation  $(\rho, \theta, \phi)$  into position in respective cartesian axis using standard relations. In the second case, the state model is proposed directly in the polar frame with the three linear independent observations  $\rho, \theta, \phi$ . By doing so, the scalar function approximation scheme proposed in [2] can be applied.

## 2 Glint Noise Generation

In radar target applications, the observation noise often is non-Gaussian. Changes in the target aspect with respect to the radar can cause the apparent center of radar reflections (direction “seen” by the antenna) to wander significantly. The random wandering of the apparent radar reflecting center gives rise to noisy or jittered angle tracking. This form of measurement noise is called angle fluctuations or target glint. Glint affects the measurement components (mostly the angles) by producing heavy-tailed, non-Gaussian disturbances, which might severely affect the tracking accuracy.

It is well documented in the literature that the so-called “glint noise” possesses the characteristics of a long-tailed distribution. Performance of conventional minimum mean square estimators (Kalman filter) can be seriously degraded if non-Gaussian noise is present. Therefore, it is of paramount importance to have accurate modeling of the non-Gaussian noise phenomenon prior to the development of any efficient tracking algorithm. Many different models have been used for the non-Gaussian glint noise present in target tracking applications. In the tail region, the plot deviates from linearity and indicates a non-Gaussian, long-tailed character. The data in the tail region are essentially associated with the glint spikes and are considered to be outliers. These outliers have a considerable influence on conventional target tracking filters, such as the Kalman filter. The effect of the glint spikes is even greater on the sample variance used in the derivation of the filter’s gain.

The glint spikes can be modeled as a Gaussian noise with large variance, resulting in an overall glint noise model which can be considered as a Gaussian mixture

with the two components used to model the background Gaussian noise and the glint spikes (Laplacian noise), respectively as shown in the figure 2.1. The weighting coefficient (glint probability) in the mixture (percentage of contamination) can be used to model the non-Gaussian nature of the glint spikes.

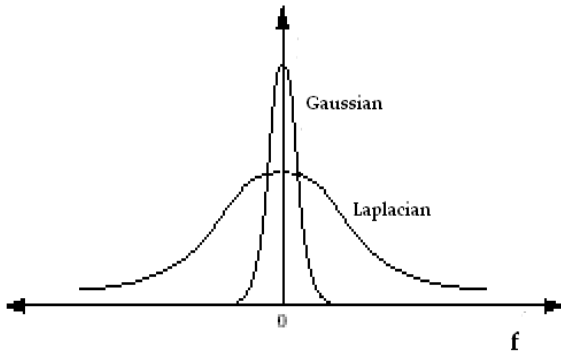


Figure 2.1: Probability distribution function of Gaussian and Laplacian noise

Therefore, the glint noise model can be generated as the mixture of two Gaussian distributions, each with a zero mean and with a fixed variance. A typical glint noise is generated with  $\sigma_G=1$  and  $\sigma_L=4$  and glint probability  $\varepsilon=0.8$ . Following algorithm [4] is used to generate Gaussian, Laplacian and Glint noise (as a mixture of both Gaussian and Laplacian noise) in MATLAB.

*Gaussian noise:*

$$w = \text{randn}(1000,1)$$

$$w_g = \sigma_G * (\psi - \bar{w}) / \sigma_w$$

where

$\bar{w}$  and  $\sigma_w$  are the mean and standard deviation of  $w$

*Laplacian noise:*

(at each sample  $k$ , where  $k= 1,2, \dots, 1000$ )

$$x = \text{randn}$$

$$y = \sqrt{0.5} * \log\left(\frac{1}{1-x}\right)$$

$$z = 2 * \text{randn} - 1$$

$$\text{if } z > 0.0 \text{ then } y = -y$$

$$w_l(k) = \sigma_L * y$$

*Glint noise:*

$$w_{gl}(k) = (1 - \varepsilon) * w_g(k) + \varepsilon * w_l(k)$$

$$k = 1,2, \dots, 1000$$

Probability density function (pdf) for Gaussian and Glint noise are computed using MATLAB function 'hist'.

Figure 2.2 shows the glint noise generated using above algorithm. The spiky pattern of glint noise manifest itself in the long tailed distribution.

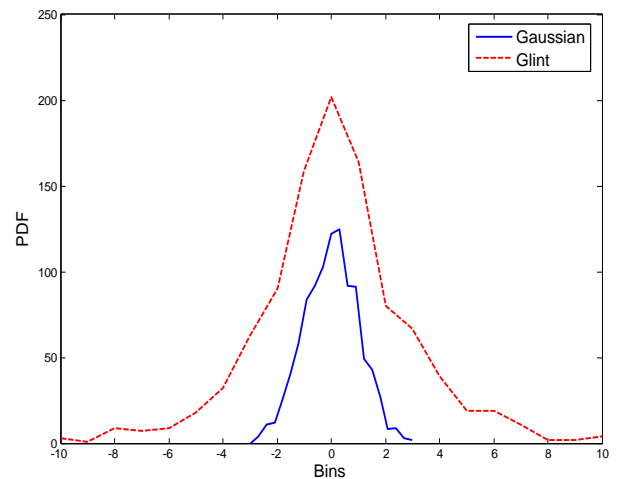
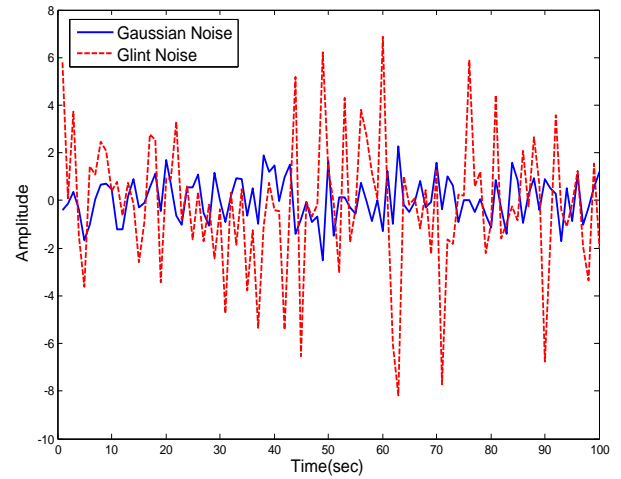


Figure 2.2: Gaussian and Glint noise and their pdf

### 3 Implementation of Masrelez filter

While the scheme proposed by Masrelez is promising, the implementation of score function is practically difficult except for simple cases. The score function implementation problem is recently solved by Wu[2]. The method employs an adaptive normal expansion to expand the score function and truncates the higher order terms in the expanded series. Consequently, the score function can be approximated by a few central moments of the observation prediction density. The normal expansion is made adaptive by using the concept of conjugate recentering and the saddle point method. However, it is shown in [2] that, though the approximation is satisfactory and the method is simple and practically feasible it is easy to implement only for the scalar observation. But the radar observation is often not scalar.

In this work the approximation score function evaluation method mentioned in [2] is extended to radar vector

observation. The non-Gaussian (glint) noise present in radar measurements is modeled as a mixture of Gaussian noise and Laplacian noise with mixing glint probability  $\varepsilon$ . Following sub sections give implementation aspects of Masreliez filter

### 3.1 Filter initialization

$\hat{X}$  : Initial filter state  
 $\hat{P}$  : Initial filter state error covariance

### 3.2 Time update

$$\tilde{X}_{(k+1)} = \Phi \hat{X}_k \quad (3.1)$$

$$\tilde{P}_{(k+1)} = \Phi \hat{P}_{(k)} \Phi^T + G_n Q G_n^T \quad (3.2)$$

where  $\Phi$  the state transition matrix  
 $Q$  the process noise covariance  
 $G_n$  the process noise gain matrix

### 3.3 Measurement update – for scalar measurements

$$\hat{X}_{(k+1)} = \tilde{X}_{(k+1)} + \tilde{P} H^T g(Z_{m(k+1)}) \quad (3.3)$$

$$\hat{P}_{(k+1)} = \tilde{P}_{(k+1)} - \tilde{P}_{(k+1)} H^T G(Z_{m(k+1)}) H \tilde{P}_{(k+1)} \quad (3.4)$$

where,  $H$  is the observation matrix and is unity for scalar observation  
 $g(\cdot)$  is the score function,  
 $G(\cdot)$  is jacobian matrix, and  
 $Z_m$  is the sensor measurement.

Following steps are required to compute  $g(\cdot)$  and  $G(\cdot)$ :

Step1:

Innovation covariance for Gaussian noise

$$S_1 = H \tilde{P} H^T + \sigma_G^2 \quad (3.5)$$

Innovation covariance for Laplacian noise

$$S_2 = H \tilde{P} H^T + 2\sigma_L^2 \quad (3.6)$$

Innovation sequence at  $k+1^{th}$  scan

$$\mu = Z_{m(k+1)} - H \tilde{X}_{(k+1)} \quad (3.7)$$

where

$\sigma_G$  is the standard deviation of the Gaussian component of the measurement (glint) noise

$\sigma_L$  is the standard deviation of the Laplacian component of the measurement (glint) noise

Step2:

$$[pdf\_gauss, g\_gauss, G\_gauss] = scfgl(S1, \sigma_G, \mu, \tilde{P})$$

$$[pdf\_Laplc, g\_Laplc, G\_Laplc] = scfgl(S2, \sigma_L, \mu, \tilde{P})$$

where ‘scfgl’ is the MATLAB function to compute pdf (probability density function), g (score function) and G (jacobian matrix) for Gaussian and Laplacian noises.

$$g(Z_m) = w_1 * g\_gauss + w_2 * g\_Laplc \quad (3.8)$$

$$G(Z_m) = w_1 * (G\_gauss - g\_gauss^2) + w_2 * (G\_Laplc - g\_Laplc^2) + g(Z_m)^2 \quad (3.9)$$

where

$$w_1 = \frac{\varepsilon * pdf\_gauss}{\varepsilon * pdf\_gauss + (1-\varepsilon) * pdf\_Laplc} \quad (3.10)$$

$$w_2 = \frac{(1-\varepsilon) * pdf\_Laplc}{\varepsilon * pdf\_gauss + (1-\varepsilon) * pdf\_Laplc} \quad (3.11)$$

The [pdf\_gauss, g\_gauss, G\_gauss] and [pdf\_Laplc, g\_Laplc, G\_Laplc] are computed within the function ‘scfgl’ as follows.

$$g\_gauss = T + \frac{Vs3(T)}{2 * (Vs2(T))^2} \quad (3.12)$$

$$G\_gauss = \frac{1}{Vs2(T)} \left[ 1 + \frac{Vs4(T)}{2 * (Vs2(T))^2} - \frac{Vs3(T)^2}{(Vs2(T))^3} \right] \quad (3.13)$$

$$pdf\_gauss = \frac{1}{\sqrt{2\pi * Vs2(T)}} e^{-\frac{(\tilde{P}^* T^2 - T * \mu)}{2}} \quad (3.14)$$

where saddle point ‘T’ is computed using ‘fzero’ function in MATLAB and

$$y_{vgt} = \mu - \tilde{P} * T$$

$$Vs2 = (y_{vgt})^2 + \frac{\mu}{T}$$

$$Vs3 = (y_{vgt})^2 + (2 * \mu - 2 * \tilde{P} * T + \frac{3}{T})$$

$$Vs4 = 6 * (y_{vgt})^4 + \frac{12}{T} * (y_{vgt})^3 + \frac{3}{T^2} * (y_{vgt})^2$$

Also pdf\_Laplc, g\_Laplc, G\_Laplc are computed in a similar way,.

Table 3.1 gives the equations of Kalman filter and Masreliez filter. The function g(.) is called the score function. It is this score function g(.) that dictates how to modify Kalman filter in the non-gaussian environment. The score function g(.) will de-emphasize the influence of large residuals when the observation prediction density is long tailed, and on the other hand, emphasize the large residuals when the observation

prediction density is short tailed. The Masreliez filter is reduced to standard Kalman filter if the initial state and noise sequences  $w_k$  and  $v_k$  (for all k) are gaussian.

Table 3.1: Comparison of Kalman filter and Masreliez Filter

<b>Kalman filter</b>	<b>Masreliez filter</b>
<b>Time update:</b> $\tilde{X}_{(k+1)} = \Phi \hat{X}_{(k)}$ $\tilde{P}_{(k+1)} = \Phi \hat{P}_{(k)} \Phi^T + G_n Q G_n^T$	<b>Time update:</b> $\tilde{X}_{(k+1)} = \Phi \hat{X}_{(k)}$ $\tilde{P}_{(k+1)} = \Phi \hat{P}_{(k)} \Phi^T + G_n Q G_n^T$
<b>Measurement update:</b> $\hat{X}_{(k+1)} = \tilde{X}_{(k+1)} +$ $\tilde{p}_{(k+1)} H^T$ $(H \tilde{P}_{(k+1)} H^T + \sigma^2)^{-1}$ $(Z_{(k+1)} - H \tilde{X}_{(k+1)})$ $\tilde{P}_{(k+1)} = \tilde{P}_{(k+1)} -$ $\tilde{P}_{(k+1)} H^T$ $(H \tilde{P}_{(k+1)} H^T + \sigma^2)^{-1}$ $H \tilde{P}_{(k+1)}$	<b>Measurement update:</b> $\hat{X}_{(k+1)} = \tilde{X}_{(k+1)} +$ $\tilde{p}_{(k+1)} H^T g(Z_{(k+1)})$ $\tilde{P}_{(k+1)} = \tilde{P}_{(k+1)} -$ $\tilde{P}_{(k+1)} H^T G(Z_{(k+1)})$ $H \tilde{P}_{(k+1)}$

Analogy between Kalman filter and Masreliez Filter

$$g(Z_{(k+1)}) \approx (H \tilde{P}_{(k+1)} H^T + \sigma^2)^{-1} (Z_{(k+1)} - H \tilde{X}_{(k+1)})$$

$$G(Z_{(k+1)}) \approx (H \tilde{P}_{(k+1)} H^T + \sigma^2)^{-1}$$

#### 4 Radar Data Simulation

To compare the performance of Masreliez filter with that of conventional Kalman filter, radar tracking measurements are simulated in the presence of glint noise. This and following sections give the details of the radar data simulation, estimation of target position from this data using Kalman filter and Masreliez filter and comparison of their performance in the presence of non-Gaussian glint noise.

Tracking radar generally measures the target position in polar coordinate system. Following state space model is used to simulate the target's position in polar frame.

State equation:

$$\tilde{X}_{(k+1)} = \Phi \hat{X}_{(k)} + G_n w_{(k)} \quad (4.1)$$

where

state vector is defined as  $X = [\dot{\rho} \ \theta \ \dot{\theta} \ \phi \ \dot{\phi}]^T$

state transition matrix is defined as

$$\Phi = \begin{bmatrix} 1 & T & 0 & 0 & 0 & 0 \\ 0 & 1 & 0 & 0 & 0 & 0 \\ 0 & 0 & 1 & T & 0 & 0 \\ 0 & 0 & 0 & 1 & 0 & 0 \\ 0 & 0 & 0 & 0 & 1 & T \\ 0 & 0 & 0 & 0 & 0 & 1 \end{bmatrix} \quad (4.2)$$

process noise gain matrix is defined as

$$G_n = \text{diag} \left[ \frac{T^2}{2} \quad T \quad \frac{T^2}{2^* \rho} \quad \frac{T}{\rho} \quad \frac{T^2}{2^* \rho^* \cos \phi} \quad \frac{T}{\rho^* \cos \phi} \right] \quad (4.3)$$

Measurement equation:

$$Z_{(k+1)} = H \tilde{X}_{(k+1)} + v_{(k+1)} \quad (4.4)$$

where

$$\text{measurement vector is defined as } Z = [\rho \ \theta \ \phi]^T \quad (4.5)$$

observation matrix is defined as

$$H = \begin{bmatrix} 1 & 0 & 0 & 0 & 0 & 0 \\ 0 & 0 & 1 & 0 & 0 & 0 \\ 0 & 0 & 0 & 0 & 1 & 0 \end{bmatrix} \quad (4.6)$$

subscript  $k$  indicates the discrete sample no.

The process noise  $w$  is generated as white noise with zero mean and gaussian distribution. The measurement noise  $v$  is generated as non-Gaussian glint noise (see section 2) with

$$\sigma_G = \begin{bmatrix} .0 & 0.004 & 0.004 \end{bmatrix}$$

$$\sigma_L = \begin{bmatrix} .0 & 0.02 & 0.02 \end{bmatrix} \text{ and with glint probability } \varepsilon = 0.9.$$

The Figures 4.1 show the simulated target  $\rho$ ,  $\theta$ ,  $\phi$  trajectories (as measured by the radar) in the presence of non-Gaussian glint noise. This simulated radar measurement data is subsequently used for tracking the target by Kalman filter and Masreliez filter using the tracking models mentioned below.

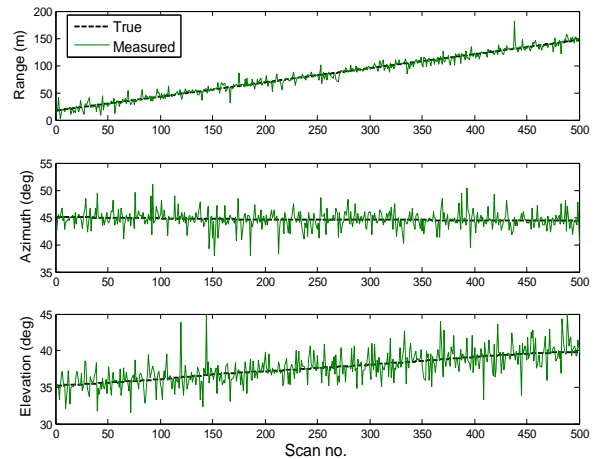


Figure 4.1: Simulated radar measurements

### 5 Tracking Models

#### 5.1 Tracking in Cartesian frame:

For tracking convenience often the radar measurements  $\rho$ ,  $\theta$ ,  $\phi$  are converted into cartesian frame (X,Y,Z axis)

as  $x_{pos}$ ,  $y_{pos}$ ,  $z_{pos}$  using the standard relation given in equation 5.1 and the target is tracked in cartesian frame with  $x_{pos}$ ,  $y_{pos}$ ,  $z_{pos}$  as observation [5,6].

$$\begin{aligned} x_{pos} &= \rho * \cos\phi * \cos\theta \\ y_{pos} &= \rho * \cos\phi * \sin\theta \\ z_{pos} &= \rho * \sin\phi \end{aligned} \quad (5.1)$$

Following state space model is used to track the target in cartesian frame.

State equation:

$$\tilde{X}_{(k+1)} = \Phi \hat{X}_{(k)} + G_n w(k)$$

Measurement equation:

$$Z_{(k+1)} = H\tilde{X}_{(k+1)} + v(k+1)$$

where

state vector is defined as

$$X = \begin{bmatrix} x_{pos} & x_{vel} & y_{pos} & y_{vel} & z_{pos} & z_{vel} \end{bmatrix}^T$$

and state transition matrix is defined as in equation (4.2)

Process noise gain matrix is defined as

$$G_n = \text{diag} \left[ \frac{T^2}{2} \quad T \quad \frac{T^2}{2} \quad T \quad \frac{T^2}{2} \quad T \right] \quad (5.2)$$

Observation matrix is defined as in equation (4.6)

$$\text{Measurement vector is } Z = \begin{bmatrix} x_{pos} & y_{pos} & z_{pos} \end{bmatrix}^T$$

Masreliez filter is implemented as per the equations given in section 3.

The process noise covariance is chosen as

$$Q = \text{diag} [3.6 \quad 2.0 \quad 3.6 \quad 2.0 \quad 3.6 \quad 2.0]; \quad (5.3)$$

The standard deviation of gaussian component  $\sigma_G = \begin{bmatrix} 1 & 1 \end{bmatrix}$ , standard deviation of laplacian component  $\sigma_L = \begin{bmatrix} 5 & 5 \end{bmatrix}$  and mixing probability  $\varepsilon = 0.9$  is chosen in the computation of the score function  $g(\cdot)$  and Jacobian matrix  $G(\cdot)$

For Kalman filter, the measurement noise matrix is chosen as:

$$R = \text{diag} \begin{bmatrix} \varepsilon * \sigma_G^2(1) + (1-\varepsilon) * \sigma_L^2(1) \\ \varepsilon * \sigma_G^2(2) + (1-\varepsilon) * \sigma_L^2(2) \\ \varepsilon * \sigma_G^2(3) + (1-\varepsilon) * \sigma_L^2(3) \end{bmatrix} \quad (5.4)$$

## 5.2 Tracking in Polar frame:

For tracking the target in polar frame, the simulated radar measurements  $\rho$ ,  $\theta$ ,  $\phi$ , are directly used as observation in the following model.

State equation:

$$\tilde{X}_{(k+1)} = \Phi \hat{X}_{(k)} + G_n w(k)$$

Measurement equation:

$$Z_{(k+1)} = H\tilde{X}_{(k+1)} + v(k+1)$$

where

state vector is defined as  $X = \begin{bmatrix} \rho & \theta & \dot{\theta} & \phi & \dot{\phi} \end{bmatrix}^T$ ,

state transition matrix is defined as in equation (4.2),

process noise gain matrix is defined in (4.3),

observation matrix is defined as in equation (4.6),

the measurement vector is  $Z = \begin{bmatrix} \theta & \phi \end{bmatrix}^T$ ,

the process noise covariance is chosen as

$$Q = \text{diag}[1.0 \quad 0.1 \quad 0.01 \quad 0.0001 \quad 0.01 \quad 0.0001];$$

The standard deviation of gaussian component,

$\sigma_G = \begin{bmatrix} 0.004 & 0.004 \end{bmatrix}$ , standard deviation of

laplacian component  $\sigma_L = \begin{bmatrix} 0.02 & 0.02 \end{bmatrix}$  and

mixing probability  $\varepsilon = 0.9$  are chosen in the computation

of the score function  $g(\cdot)$  and Jacobian matrix  $G(\cdot)$

Similarly for Kalman filter, the measurement noise is chosen as given in equation (5.4):

## 6 Results and Discussion

The results are compiled from 100 monte carlo runs from both the Kalman filter and Masreliez filter using both the Cartesian and polar tracking models.

### 6.1 Tracking in Cartesian frame:

Figures 6.1 to 6.3 show the trajectory match from both the filters in each axes respectively. From these trajectory match it can be seen that the trajectories estimated from Masreliez filter is relatively closure to the corresponding true trajectories.

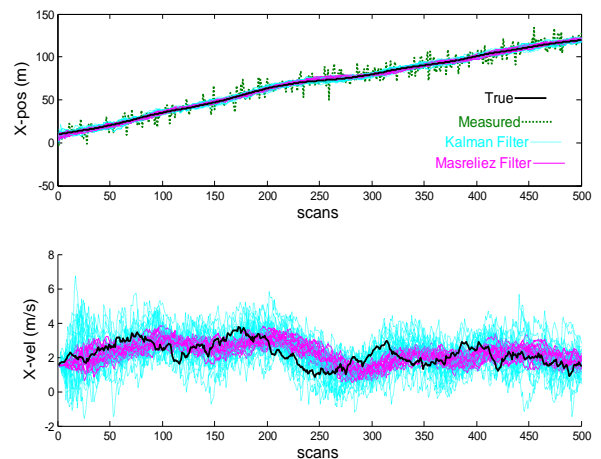


Figure 6.1: Filtered X-position and velocity trajectories

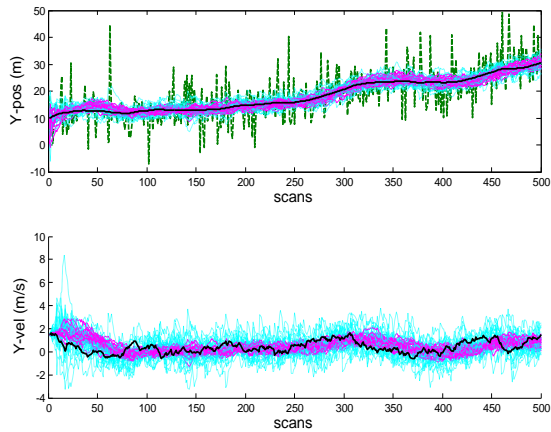


Figure 6.2: Filtered Y-position and velocity trajectories

Figure 6.4 shows the filter residuals with bounds. The bounds are computed as  $\pm\sqrt{H\tilde{P}H^T+R}$ . If the 95% of the filter error is within these bounds, it is expected that the filter is performing optimally[7]. Therefore, from the figure 6.4 it is clear that the performance of the Masreliez filter is relatively better than the Kalman filter.

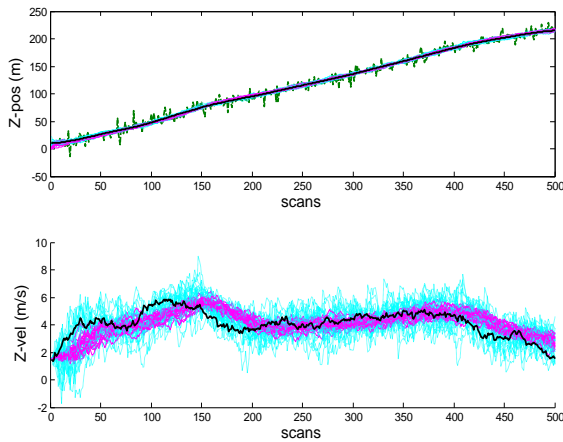


Figure 6.3: Filtered Z-position and velocity trajectories

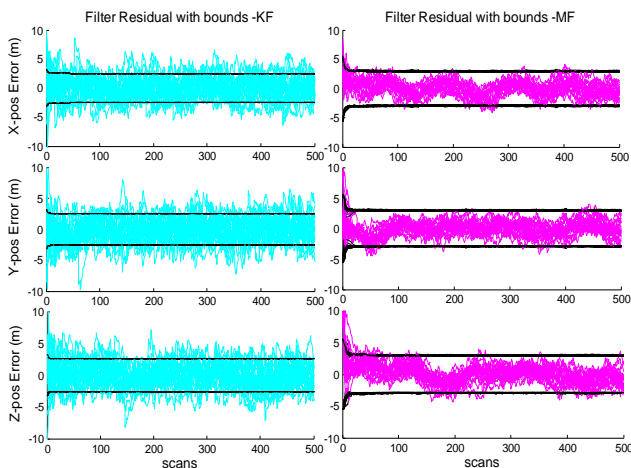


Figure 6.4: Residual with bounds

Figure 6.5 shows the score function  $g(\cdot)$  and  $G(\cdot)$  evaluated for all the three observables. In Masreliez filter, it is this score function  $g(\cdot)$  that dictates how to modify the Kalman filter in the non-Gaussian noise. From the figure 6.5, it is clear that the score function  $g(\cdot)$  operating on innovation sequence will emphasize the correction factor to be added to the model prediction during gaussian region. Whereas during the non-gaussian region, the score function remains constant and hence applies a constant correction factor on the model predicted output.

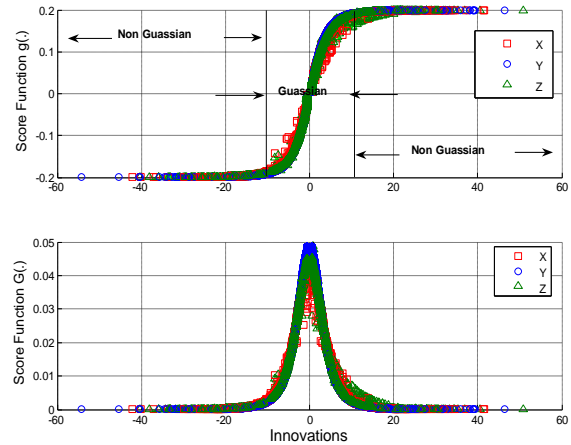


Figure 6.5: Score function from Masreliez filter

When the intensity of glint noise in the observation is reduced, the Kalman filter seems to be performing satisfactorily. Figure 6.6 shows the performance of Kalman and Masreliez filter when the glint noise is mild (glint probability  $\epsilon$  reduced from 0.9 to 0.3) in the observation.

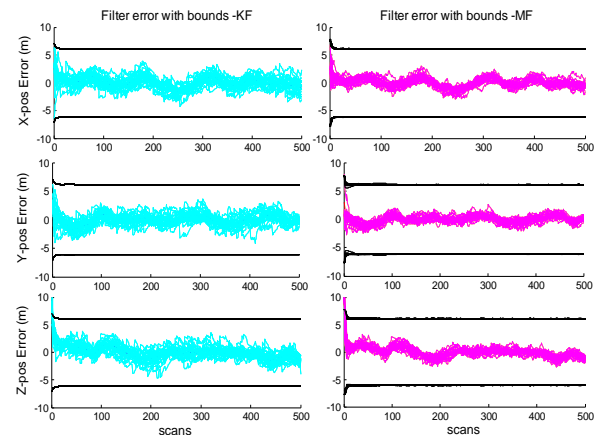


Figure 6.6: Residual with bounds ( $\epsilon = 0.3$ )

## 6.2 Tracking in Polar frame:

Figures 6.7 to 6.9 show the trajectory match from both the filters. Figure 6.10 shows the residual with bounds. As in the previous case, the performance of the Masreliez filter is relatively better than that of Kalman filter in the presence of significant glint noise ( $\epsilon = 0.9$ ) in the observation.



## 7 Concluding Remarks

In this paper, Masreliez filter which is a Kalman type of recursive filtering scheme that can work nearly optimally in the presence of glint, is implemented. The main computation in Masreliez filter is to evaluate the score function which directly influences the estimates of the target states. An efficient approximation method for score function evaluation developed by Wu[2,3] is extended to radar vector observation.

The simulation studies have shown that the performance of the Masreliez filter is relatively better than that of the conventional Kalman filter in the presence of significant glint noise in the observation. However, when the glint effect is mild (i.e. when the glint probability  $\epsilon < 0.5$ ) in the measurement noise, the performance of the Kalman filter seems to be also satisfactory.

## 8 References

- [1] Masreliez C J, *Approximate non-Gaussian filtering with linear state and observation relations*, IEEE Transactions on Automatic Control, Vol. 20, pp 107-110, Feb 1975.
- [2] Wu W R, *Kalman filtering in non-Gaussian environment using efficient score function approximation*, In proceedings of 1989 IEEE International Symposium on Circuits and Systems, 1989, 413-416.
- [3] Wu W, *Target tracking with glint noise*, IEEE Transaction on Aerospace and Electronic Systems, Jan 1993, Vol 29, pp 174-185.
- [4] Sudesh K and Raol J R, *Fuzzy logic based adaptive filter for target tracking in the presence of glint noise*, NAL PD FC 2004, October 2004.
- [5] Yaakov Bar-Shalom and Xiao-Rong Li, *Multi target – Multi sensor tracking: Principles and Techniques*, YBS publications, 1995.
- [6] Sudesh K, Girija G and Raol J R, *Evaluation of converted measurements and modified extended Kalman filters for target tracking*, AIAA GNC conference and exhibit, Austin, Texas (USA), Aug 2003, AIAA paper no. 2003-5450
- [7] Candy J V, *Signal Processing: The Model Based Approach*, McGraw Hill International Edition, Singapore, 1987

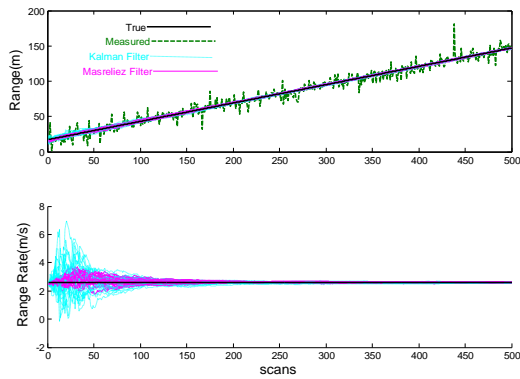


Figure 6.7: Filtered range and range rate trajectories

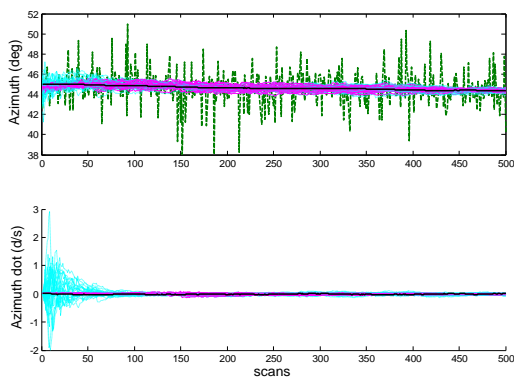


Figure 6.8: Filtered azimuth and azimuth rate trajectories

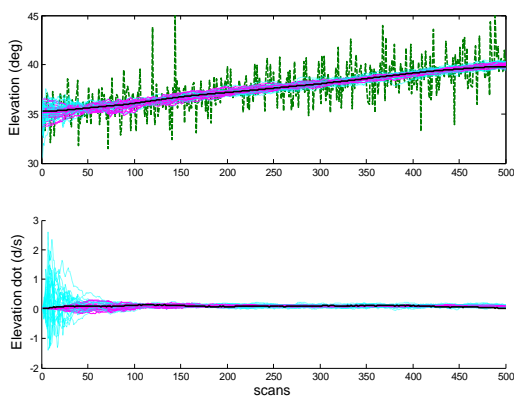


Figure 6.9: Filtered elevation and elevation rate trajectories

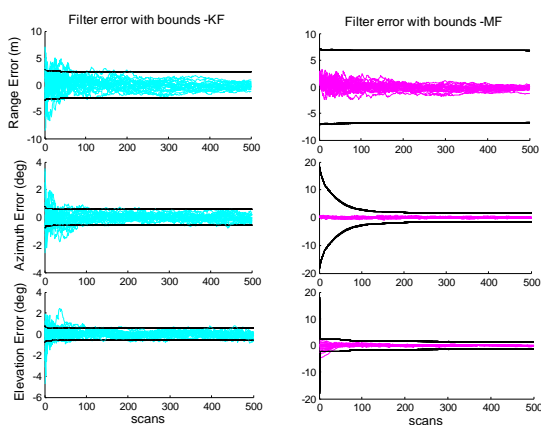


Figure 6.10: Residual with bounds